Enhancement of the inertial navigation system for the Morpheus autonomous underwater vehicles

Article *in* IEEE Journal of Oceanic Engineering · November 2001

DOI: 10.1109/48.972091 · Source: IEEE Xplore

Enhancement of the Inertial Navigation System for the Morpheus Autonomous Underwater Vehicles

Gabriel Grenon, P. Edgar An, Samuel M. Smith, and Anthony J. Healey

***Abstract*—This paper presents the design and development of an enhanced inertial navigation system that is to be integrated into the Morpheus autonomous underwater vehicle at Florida Atlantic University. The inertial measurement unit is based on the off-the-shelf Honeywell HG1700-AG25 3-axis ring-laser gyros and three-axis accelerometers and is aided with ground speed measurements obtained using an RDI Doppler-velocity-log sonar. An extended Kalman filter has been developed, which fuses together asynchronously the inertial and Doppler data, as well as the differential global positioning system positional fixes whenever they are available. A complementary filter was implemented to provide a much smoother and stable attitude estimate. Thus far, preliminary study has been made on characterizing the inertial navigation system-based navigation system performance, and the corresponding results and analyzes are provided in this paper.**

***Index Terms*—Autonomous underwater vehicles, inertial navigation, Kalman filtering, underwater navigation.**

I. Introduction

AUTONOMOUS underwater vehicles (AUVs) are unmanned and untethered submarines. They provide marine researchers with a simple, long-range and low-cost solution with which to gather oceanographic data [8]. Common applications for deploying AUVs include oceanographic sampling, bathymetry profiling, underwater system inspection, and military mine counter measure (MCM) operations [2], [20], [22], [24]. In many of these missions, it is critical that the vehicle position be known precisely and in real time such that the seafloor can be mapped accurately and bottom mines reacquired with a high degree of confidence. Underwater navigation for AUVs is thus a very challenging research topic and a major subject of concern to both the AUV community and their end users.

Apart from the vehicle design and development cost, the operational cost primarily dictates the practicality of AUVs for commercial and military use. Rapid development on sensors and electronics technology in the past decade has made it possible that smaller, better-performing and lower power AUVs can be built [1], [21], [25], [26]. This has an important strategic advantage. Smaller AUVs typically require fewer crew and smaller boat support for launch, recovery, and tracking, thereby significantly reducing the operational cost per distance traveled. It is anticipated that the trend of miniaturizing AUVs will continue in the future. To further capitalize on this output, operations that involve a fleet of small (communicative) AUVs become financially possible [23].

In smaller AUVs, there is less space to install payload or vehicle-specific instruments onboard. To make matters worse, smaller AUVs generally suffer from larger vehicle motion especially in a highly energetic environment. It is thus important that these constraints be considered when designing a small AUV otherwise the usefulness of the collected scientific data might be jeopardized. This paper is focused on the navigation aspect for small AUVs.

For air or ground vehicles, the Global Positioning System (GPS) with differential corrections (DGPS) can provide very precise and inexpensive measurements of geodetic coordinates [18]. With the recent removal of the intended Selective Availability interference, typical GPS position error is now on the order of 10 to 20 m. Unfortunately, these radio signals cannot penetrate beneath the ocean surface, and this poses a considerable constraint on the overhead of a vehicle mission, which is surfacing to obtain GPS fixes. One alternative solution for autonomous underwater navigation is to make use of an array of long-base-line (LBL) acoustic beacons such that the vehicle position can be estimated by means of triangulation [3]. The LBL solution requires the beacon array to be either mounted on the ocean bottom or moored on the surface (inverted LBL), and thereby restricts the AUV coverage area to be within the beacon grid. In addition, the performance of this externally aided positioning depends largely on the sound-speed profile in the water column. For multiple AUV operations, independent sets of beacons must be installed, and this rapidly increases the logistical complexity of a mission [23].

Dead reckoning (DR) aided with Doppler velocity measurement has been, and remains, the most common method for underwater navigation. In the DR mode, the vehicle relies on its set of navigation instruments to estimate the vehicle's position. These instruments include a three-axis accelerometer and gyroscope, a flux-gate compass, and a Doppler-velocity-log (DVL) sonar. The system is commonly referred to as a Doppler-aided inertial navigation system (INS) as most of these instruments rely on the inertial properties of gravity and magnetic field. The DR solution does not measure directly the vehicle's position, but instead estimates it by integrating the velocity and bearing measurements with respect to time. Any measurement errors in velocity and heading will thus result in a growing position error, up to a threshold beyond which the navigation performance becomes unacceptable.

The Department of Ocean Engineering at Florida Atlantic University (FAU) has developed an enhanced INS for its new

Manuscript received October 12, 2001; revised June 7, 2001. This work was supported by the Office of Naval Research under Grant N00014-96-1-5029.

G. Grenon, P. E. An, and S. M. Smith are with the Institute of Ocean and Systems Engineering - SeaTech, Florida Atlantic University, Dania, FL 33004 USA.

A. J. Healey is with the Department of Mechanical Engineering, Naval Postgraduate School, Monterey Beach, CA 93943 USA.

Publisher Item Identifier S 0364-9059(01)10368-7.

generation of small AUV (dubbed Morpheus) [21]. This navigation system consists of a Honeywell Inertial Measurement Unit (IMU), together with a GPS/DGPS receiver (by Motorola and CSI, respectively), a TCM2 flux-gate compass, and a DVL sonar (by RD Instruments, Inc.). A navigation system is commonly referred to as INS when it uses only inertial sensors to estimate its attitude, velocity, and position. Besides gyroscopes and accelerometers, our system makes extensive use of DVL and GPS data and would be more appropriately labeled as Doppler-aided/GPS-aided INS. However, for simplicity, for the remainder of this paper we will simply refer to the Morpheus navigation system as INS.

A suite of data fusion and correction methods that combine all available asynchronous measurements has been implemented [11]. These methods include a complementary filter for estimating the vehicle attitude, a deviation table for correcting the compass bias, and an extended Kalman filter for estimating the vehicle position and heading [7], [16]. With improved underwater navigation accuracy, the overall performance of a mission can be made more efficient because it requires fewer surfacing maneuvers (for acquiring GPS fixes) for a given position-error tolerance.

In the remainder of the paper, the characteristics of the sensors used in the Morpheus INS are first reviewed, followed by a description of the filtering algorithms. Finally, practical results assessing the performance of the INS are discussed and concluding remarks are drawn.

II. Navigation System Instruments

In this section, the navigation instruments and their characteristics on the Morpheus are presented.

A. Inertial Measurement Unit (IMU)

An IMU consists of a three-axis gyroscope and a three-axis accelerometer. A single-axis gyroscope measures the angular rate of change of a platform about its main axis of rotation whereas a single-axis accelerometer measures the linear acceleration of a platform together with the gravity along its axis of translation. Both sensors measure the motion relative to an inertial frame of reference.

Four gyroscope technologies are available: mechanical, solid-state, fiber-optic (FOG), and ring-laser (RLG). A mechanical gyroscope uses the inertia of a very fast spinning ball to detect any angular change about its axis. Despite their high reliability and accuracy, these mechanical sensors are not currently adapted for small AUVs (5–10 ft in length) because they are cumbersome, consume much power, and can generate undesired mechanical vibrations. Solid-state gyros are operated based on the principle of the Coriolis effect: when a translating body is subject to angular rotation, the Coriolis force experienced is proportional to an applied angular rate [4], [14]. The operational principles for both FOGs and RLGs are very similar to each other and are explained in the following. Two beams (laser or light) are sent in opposite directions in a closed beam path. Mirrors in RLGs or a fiber-optic cable in FOGs are used to bend the beam so that it follows a closed path. If the platform on which a gyro is mounted is at rest, the two beams will have identical frequencies at the end of each loop. When a gyro experiences an angular motion about its axis of rotation, the traveled path length of one beam increases while that of the other decreases, resulting in a Doppler shift which is directly proportional to the angular rate. Both FOGs and RLGs can be inexpensive, low power, and small and have excellent reliability and stability performances. It should be noted that a long-term drift error is common to both an FOG and an RLG, and the bias magnitude (or the unit cost) is primarily determined by the length of the beam path and its sensitivity to temperature variation.

TABLE I
Performance Comparison of Gyros and Accelerometers

Type	Sub-Type	Bias Stability
Gyro	Mechanical	[0.000015 – 0.001] °/hr
	Solid-State	[1 – 3600] °/hr
	RLG	[0.001 – 15] °/hr
	FOG	[1.0 – 150] °/hr
Accelerometer	Mechanical	[0.05 – 5] μg
	Quartz Resonator	[100 – 10,000] μg

TABLE II
Characteristics of the HG1700AG25 Honeywell IMU

	RLG	RBA
Range	±1074°/sec	±37g
Resolution	$6.67*10^{-7}$°/sec	23ng
Noise	1°/hr Drift	1mg Bias
Update Frequency	100Hz	100Hz
Interface	RS422 – 115.2kbps	
Power	+5/±15VDC – 5.5W	
Dimensions	5" x 5" x 2.882"	

A wide variety of accelerometers are available on the market, such as mechanical, piezo-resistive, differential capacitive, or resonant-beam. Similar to previous descriptions of the gyroscopes, mechanical accelerometers are not commonly used in small AUVs. Typical requirements for an accelerometer are a low noise level and a small bias. Table I briefly compares these technologies in terms of their averaged bias stability performances reported in [4], although it should be cautioned that there is a large variation in performance for each of the units based on its constraint in cost and size.[1]

On the Morpheus, these sensors were packaged into a single IMU. The HG1700AG25 Honeywell IMU, which consists of three RLGs and three resonant beam accelerometers (RBAs), was selected for this application. The characteristics of the unit are described in Table II.

B. Magnetometer Compass

Most AUVs rely on a magnetic compass to provide heading information. Such instruments traditionally encompass a liquid-level-based tilt sensor and three orthogonal magnetic field sensors, thus providing roll and pitch measurements as well as heading information.

To compute heading, the magnetic measurements are first transformed from the body-fixed frame (for strapped-down

[1]The Litton LN250 IMU is listed to provide a gyro bias of 0.004°/h and an acc bias of 40 μg.

TABLE III
CHARACTERISTICS OF THE TCM2 COMPASS

Heading Information	
Accuracy	±1°
Resolution	0.1°
Repeatability	±0.1°
Range	0° - 359.9°
Magnetometer Output	
Accuracy	±0.2μT
Resolution	0.01μT
Range	±80μT
Tilt Information	
Accuracy	±0.2°
Resolution	0.1°
Repeatability	±0.2°
Range	±20°
Power Requirements	+5VDC – 0.1W
Dimensions	2.5" x 2.00" x 1.25"
Interface	RS232C
Maximum Frequency	40Hz

type) into the local-level frame [10]. The mathematical transformation is shown as

$$\begin{bmatrix} X_{\text{mag}} \\ Y_{\text{mag}} \\ Z_{\text{mag}} \end{bmatrix}_{\text{local}} = \begin{bmatrix} \cos\theta & \sin\theta\sin\phi & \sin\theta\cos\phi \\ 0 & \cos\phi & -\sin\phi \\ -\sin\theta & \cos\theta\sin\phi & \cos\theta\cos\phi \end{bmatrix} \cdot \begin{bmatrix} X_{\text{mag}} \\ Y_{\text{mag}} \\ Z_{\text{mag}} \end{bmatrix}_{\text{body}} . \quad (1)$$

The heading is then evaluated as

$$\psi = \tan^{-1}\left(\frac{-Y_{\text{mag}}}{X_{\text{mag}}}\right) * \frac{180}{\pi}\,(\circ) \quad (2)$$

where θ, ϕ, and ψ represent pitch, roll, and heading in radians and X_{mag} and Y_{mag} correspond to the two orthogonal field components expressed in the local-level frame.

The *Precision Navigation* TCM2 magnetometer compass, which is widely used within the underwater community, was selected for the Morpheus. With its internal processing of the transformation, the TCM2 is capable of outputting pitch, roll, and heading information in a strapped-down configuration. Its main characteristics are displayed in Table III.

Two major difficulties arise when dealing with the TCM2, namely the inherent low-pass response (due to the inertia of tilt sensor fluid) and heading error (due to internal and/or external magnetic anomalies).

Because of the viscosity of the sensors' liquid, the pitch and roll errors are characterized by their time lag and attenuation, and they can be significant if the instrument is subject to considerable vehicle motion, as implied from (1) and (2). In addition, the TCM2 is sensitive to local magnetic sources which can originate from the vehicle (e.g., batteries, motors and cables), or any external objects encountered in the vicinity (e.g., mines and cables). These noise sources generate either static or time-varying magnetic fields, and it is the intention in this paper that the static magnetic fields be characterized and minimized.

TABLE IV
CHARACTERISTICS OF THE RDI NAVIGATOR DVL

Available frequency		**1200kHz**	**300kHz**
Beamwidth		1.2°	3.9°
Beam angle		30°	30°
Configuration		4-beam, convex	4-beam, convex
Minimum altitude		0.5 m	1.0 m
Maximum altitude		30 m	200 m
Precision	**V=1.0 m.s^{-1}**	0.3 cm.s^{-1}	0.3 cm.s^{-1}
	V=3.0 m.s^{-1}	0.4 cm.s^{-1}	0.6 cm.s^{-1}
	V=5.0 m.s^{-1}	0.5 cm.s^{-1}	0.8 cm.s^{-1}
Accuracy (cm.s^{-1})		±0.2 % ±0.2	± 0.4 % ±0.4
Power		48VDC, 17W	48VDC, 41W
Dimensions		7.1 x 7.1 x 6"	8.8 x 8.8 x 8.2"

To calibrate the heading sensor, the TCM2 unit has an internal built-in routine, which can compensate for any hard-iron field effect on the vehicle [19]. Although this results in a better heading performance, the residual error can still be large (up to ±5°) (see Fig. 7). To improve the heading performance further, one can build a deviation table for the TCM2 although this requires an accurate heading reference during the building process. See Section IV-D for more explanation on the topic.

C. Velocity Sensor

Precise ground and water velocity measurements can be acquired underwater using a DVL sonar. A DVL transmits an acoustic ping of a specific frequency and receives returns from the ocean bottom and particulate in the water column. Any shift in frequency (Doppler shift) in the returned signals with respect to the transmitted signal is then determined in order to calculate the vehicle's velocity (forward, starboard, and vertical) expressed in the DVL frame. The frequency of transmission determines the resolution of the measurement, the transducer size, and the range. To reduce the spreading loss, the instrument uses a narrow beamwidth. Typically, a DVL error is smaller than 1% of the vehicle speed.

On the Morpheus, an RD Instruments Navigator DVL was selected to provide the body-fixed ground speed information, and the characteristics of the instrument are summarized in Table IV.

D. GPS/DGPS

The GPS uses a constellation of 24 satellites monitored from the ground to provide absolute positioning of any object on the entire planet [18]. Five widely separate ground stations continuously monitor the satellites, control and correct their trajectories, and synchronize the clocks of all satellites twice a day. From any point on the earth surface, at least four satellites (usually six) are visible at all times. Provided all satellites have a very accurate clock, and four satellites are visible from a point, a four-equation, four-unknown (x, y, z, t) system can be used to extract accurately the vehicle's position. To further improve the accuracy, a differential correction for the GPS (DGPS) can be used. In this mode, a precisely known ground station can be used to estimate the range error in the GPS signal, thus reducing the position error from about 20 m down to less than 5 m.

TABLE V
CHARACTERISTICS OF THE VP ONCORE GPS/DGPS

Acquisition time TTFF	20 s w/ ephemeris 45 s w/out ephemeris 2.5 s reacquire
Positioning accuracy	GPS < 20 m DGPS 1-5 m
Update frequency	1 Hz
Timing accuracy (1fix/sec)	130 ns
Power	5VDC, 1.1W
Dimensions	2.0 x 3.25 x 0.64"

On the Morpheus, the GPS and differential receivers were selected from Motorola VP Oncore and CSI, respectively, and the basic characteristics are summarized in Table V.

III. DATA FILTERING

The navigation algorithm performs three major filtering tasks: it estimates the pitch and roll angles, computes the vehicle heading using the magnetic field measurements and corrects for static magnetic disturbances, and finally estimates the vehicle position using an extended Kalman filter. Additional preconditioning functions include coordinate transformation of all body-fixed variables, compensation of gyroscope and accelerometer measurements for the earth rotation, estimation of gyro bias, and rescaling of the DVL output based on sound-speed measurements. Before discussing these features, the data flow structure is presented next.

A. Data Flow

The vehicle's depth and altitude sensors, namely the CTD and DVL, respectively, provide accurate depth and altitude information. Therefore, the position estimator only focuses on estimating the vehicle position on the horizontal plane.

Fig. 1 shows the structure of the INS data flow. On the top left section of the figure, a complementary filter combines the accelerometer and gyroscope data (after the latter have been transformed into the local-level plane) in order to estimate the current pitch and roll angles of the vehicle (see Section IV-C). The heading can be obtained either directly from the magnetic compass output, or integration of the gyroscope data (in this case the compass output is only used to initialize the heading). The two cases are considered and compared in Section V.

Finally the velocity, yaw rate, and heading data are combined with the GPS/DGPS measurements to feed into the extended Kalman filter. The filter main tasks are to estimate online the heading bias and vehicle position.

B. Preconditioning Functions

Before being fed to the Kalman filter, the IMU measurements must be compensated for the earth rotation and the DVL measurements corrected for the sound-speed variability.

1) Compensation of the Earth Rotation Effect on the IMU Measurements: A centripetal acceleration, which is due to the earth rotation, is sensed by the IMU accelerometers and should be removed from the measurements. Assume that the earth is spherical. At a latitude λ, the earth acceleration can be expressed as

$$a_\lambda = R_\lambda \Omega^2 = R_o . \cos\lambda . \Omega^2. \tag{3}$$

At the equator, the earth acceleration is

$$\begin{aligned} a_{\text{equ}} &= 6378.14e^3 . (7.2921e^{-5})^2 \\ a_{\text{equ}} &= 0.0339\,\text{m}\cdot\text{s}^{-2}. \end{aligned} \tag{4}$$

Note that the earth rotation component is thus about three times as large as the instrument bias and is therefore too large to be ignored.

Similarly, the earth rotation affects the gyroscope measurements, and its amplitude can be expressed as

$$\Omega = \frac{2\pi}{T} \begin{bmatrix} \cos\lambda \\ 0 \\ -\sin\lambda \end{bmatrix} \tag{5}$$

where $T = 86\,164$ s is the earth rotation period. These components must be removed from the IMU measurements before they are fed into the Kalman filter.

2) Characterization of Gyroscope Drift: A gyroscope is generally characterized by its short-term accuracy and long-term drift. The long-term drift is largely correlated with the gyroscope's ambient temperature, and it is of interest to characterize such a drift accurately so that its effect can be removed or minimized. A series of experiments was carried out to model the drift. The gyroscope was mounted on a precisely oriented platform, starting at the lowest operating temperature. It was powered up, and its outputs were logged as the internal temperature increased until it reached a steady-state equilibrium. The operation was repeated in several instances, and a best-fit approximation of the corresponding drift was computed. The results in Fig. 3 are based on the assumption that the drift varies as a function of the temperature only and does not depend on the rate of change of temperature. On average, it took 3 h to reach the steady state from a cold start.

3) Correction for Sound Velocity Variability: The DVL computes the vehicle velocity over ground based on the speed of sound, and it generally varies as a function of salinity, temperature, and density of the water. The DVL mounted on the Morpheus AUV does not have an internal CTD sensor, and thus a fixed sound-speed value of 1500 $\text{m}\cdot\text{s}^{-1}$ is assumed by the DVL processing unit. To compensate for the sound speed variability, an external CTD, which is available on Morpheus, is used to provide the correct scaling factor.

The sound speed can be estimated using the following formula [17]:

$$\begin{aligned} V_{\text{sound}} = {} & 1449.2 + 4.6T - 0.055T^2 + 0.000\,29T^3 \\ & + (1.34 - 0.01T)\cdot(S - 35) + 0.016D \end{aligned} \tag{6}$$

where V_{sound} is the speed of sound in the water ($\text{m}\cdot\text{s}^{-1}$), T is the water temperature (°C), S is the salinity (psu), and D is the depth (m).

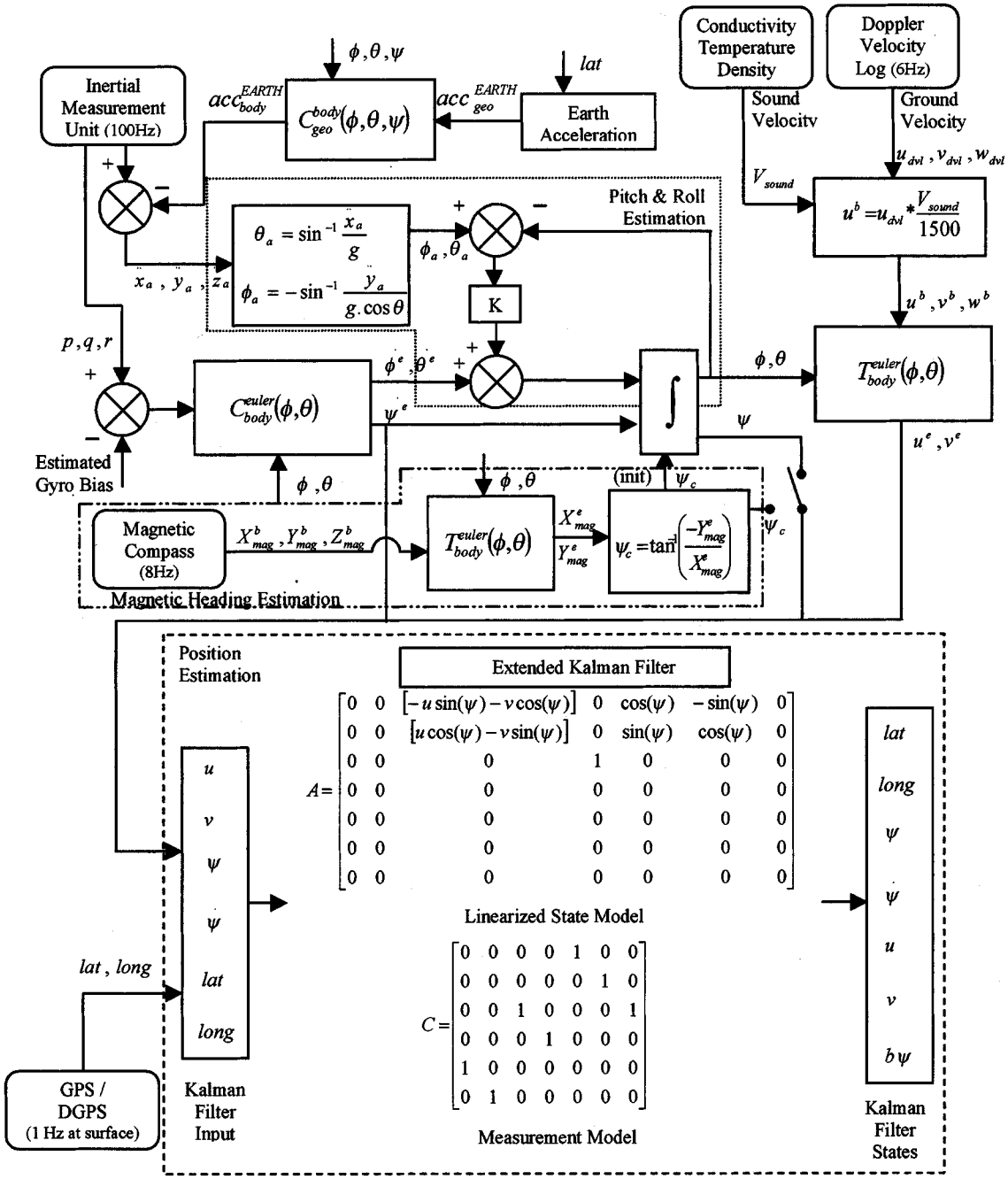

Fig. 1. INS data flow.

The DVL velocity is then corrected as

$$V_{\mathrm{DVLcorrected}} = V_{\mathrm{DVL}} \cdot \frac{V_{\mathrm{sound}}}{1500}. \tag{7}$$

C. Complementary Filter for Pitch and Roll Estimation

While the pitch and roll measurements are directly available from the TCM2, they exhibit undesired features that can have a considerable impact on navigation accuracy. These features are time lag and attenuation as well as low resolution. An alternative method to obtain better pitch and roll information is thus needed.

In cruising conditions, the only averaged force acting upon the vehicle is gravity. If the accelerations along the axes of the vehicle are known, the pitch and roll angles can be estimated as

$$\theta = \sin^{-1}\left(\frac{\ddot{x}}{g}\right) \tag{8}$$

$$\phi = -\sin^{-1}\left(\frac{\ddot{y}}{g \cdot \cos\theta}\right) \tag{9}$$

where $\ddot{x}$ and $\ddot{y}$ are the forward and starboard accelerations, respectively, θ and ϕ are the pitch and roll angles, and g is the local gravitational constant.

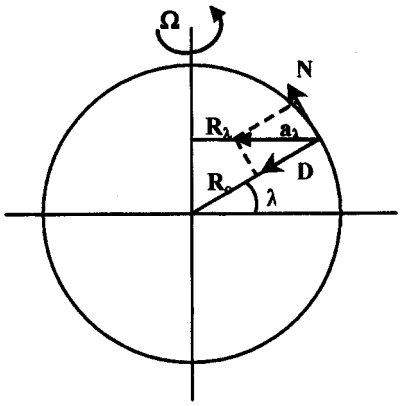

Fig. 2. Earth rotation.

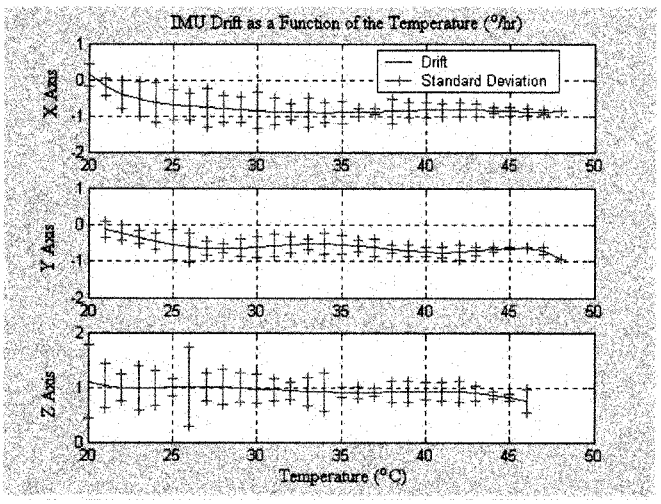

Fig. 3. Gyro drift approximation. The red bars represent the standard deviation as observed in different trials.

The Honeywell IMU RBAs guarantee high update rate (100 Hz) and high acceleration accuracy (1 mg noise) and stability, but the drawback is its relative high-frequency noise. On the other hand, the accuracy of the RLGs is limited over time by its long-term drift, but the sensors have good short-term accuracy, within the same frequency spectrum as that of the accelerometers. By combining the two data types into a complementary framework, it is possible to minimize both the high-frequency noise in the accelerometers and the low-frequency drift in the gyroscopes, resulting in a very accurate, stable, and rapidly updated attitude estimate.

The roll angle (the pitch is estimated in the same way) is estimated as [28]

$$\dot{\phi}_{\text{filter}}(t) = \dot{\phi}_{\text{gyroscope}}(t) + K \cdot (\phi_{\text{accel}}(t) - \phi_{\text{filter}}(t-1)). \tag{10}$$

Transforming the equation into the Laplace domain

$$s\phi_{filter} = s\phi_{\text{gyroscope}} + K \cdot \phi_{\text{accel}} - K.\phi_{\text{filter}} \cdot e^{-s.dt} \tag{11}$$

$$s\phi_{\text{filter}} = s\phi_{\text{gyroscope}} + K \cdot \phi_{\text{accel}} - K.\phi_{\text{filter}} \cdot (1 - s \cdot dt + \cdots) \tag{12}$$

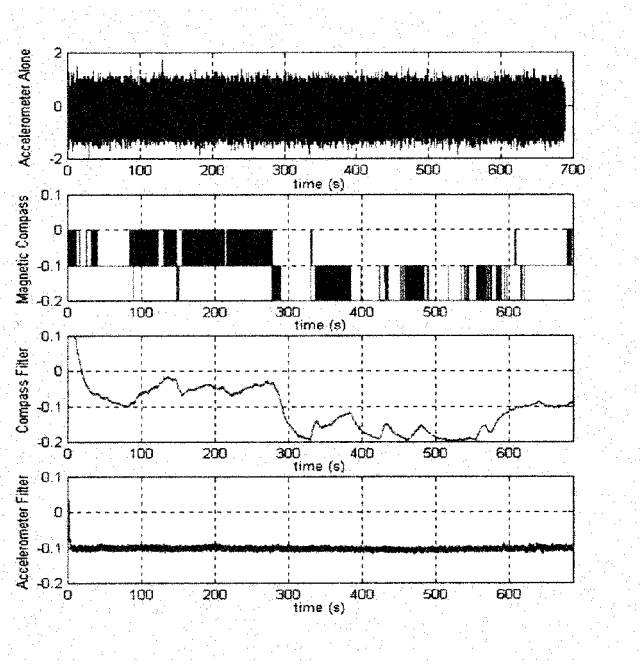

Fig. 4. Roll estimation in static conditions (°).

for dt small, the equation above can be simplified as

$$s\phi_{\text{filter}} = s\phi_{\text{gyroscope}} + K.\phi_{\text{accel}} - K \cdot \phi_{\text{filter}}. \tag{13}$$

Then

$$\frac{\phi_{\text{filter}}}{\phi_{\text{gyroscope}}} = \frac{s}{s+K} \quad \frac{\phi_{\text{filter}}}{\phi_{\text{accel}}} = \frac{K}{s+K}. \tag{14}$$

Finally, using a Euler first-order method for derivative approximation, the updated filter can be expressed as

$$\phi_{\text{filter}}(t) = \phi_{\text{filter}}(t-1) + \dot{\phi}_{\text{filter}}(t) \cdot \Delta t. \tag{15}$$

Another complementary filter can be built with the RLGs, using the roll and pitch measurements from the TCM2 tilt sensor in place of those estimated by the accelerometers. The performance of these two complementary filters was evaluated in both static and dynamic conditions [12]. Fig. 4 displays, from top to bottom, the roll angles estimated in static conditions by:

1) the accelerometers alone;
2) the TCM2 compass alone;
3) the complementary filter combining the TCM2 tilt sensor and the gyroscopes;
4) the complementary filter combining accelerometers and gyroscopes.

Obviously the accelerometers cannot be used alone to estimate the vehicle attitude because the noise level is too high. On the other hand the TCM2 roll has a low resolution. Combining either sensor above with the gyroscopes lead to better results. The complementary filter that makes use of the accelerometers provides by far the best results, being stable, with low noise and very small fluctuation ($\pm 0.01°$). High frequency noise from the accelerometers is indeed very significantly reduced, whereas the low frequency drift from the gyroscopes is removed.

When the IMU was rolled back and forth, the filter performance was found to be superior to that of the TCM2 alone, as

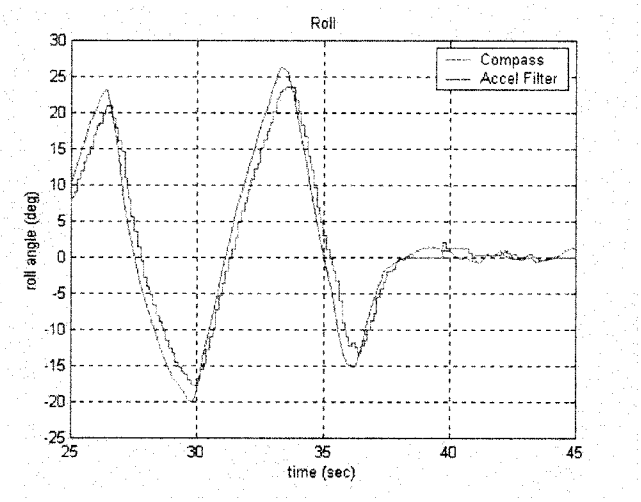

Fig. 5. Roll estimation in a moving environment (°).

Fig. 5 shows. The output given by the complementary filter is smoother, highly precise, and does not suffer from considerable attenuation and time lag, as compared to the TCM2 output.

It should be reminded that the accelerometer-based filter assumes there is no mean acceleration. When there is vehicle maneuvering, such as any significant change in speed, heading or depth, the accelerometer not only measures the gravity effect but also the acceleration induced by the vehicle. During such periods, the gyroscopes alone must be used to estimate the roll and pitch values.

D. Heading Estimation

The TCM2 heading output can have a large error in the presence of magnetic anomalies surrounding the vehicle, as well as the time lag caused by its internal tilt sensor. To minimize the time lag, the heading is computed directly from the magnetic field measurements using the estimated pitch and roll outputs, as described previously.

An experiment was set up to compare the performance when the TCM2 heading was used directly, and when the heading was calculated based on the magnetic field measurement with the improved pitch and roll estimates. In this experiment, the compass and the IMU were mounted on a common module and were carefully aligned.

Fig. 6 presents the results. Fig. 6 (a) shows the overall motion given to the module: first a slow, full 360°rotation, followed by a fast rocking motion.

Fig. 6(b) shows the direct TCM2 heading and the heading computed from the magnetic measurements, when a slow motion was given to the unit. Although the TCM2 heading was close to the computed heading, without any noticeable time lag, it was not as smooth as the computed heading, as can be seen in the rectangular boxes. This suggests that, even in smooth, slow conditions, it is desirable to compute the heading from the magnetic measurements rather than rely on the compass itself. This effect is magnified when we consider the fast rocking motion, as illustrated in Fig. 6(c) and (d). It should be noted that the staircase behaviors observed for both headings were due to the slow sampling rate of the instrument (16 Hz) with respect to the vehicle motion.

To deal with the magnetic anomalies on the vehicle, the computed TCM2 heading can be further compensated using a deviation table [13]. To generate a deviation table, we need to have an accurate heading reference available during the building process. A gyroscope, which is more accurate than the compass over a short time span, can be used as the heading reference by integrating its rate measurements over time. The process can be performed either on land or in the water, but must be away from all possible sources of magnetic noise other than those generated within the vehicle. The deviation table that we currently use on the Ocean Explorer AUV has a resolution of a one-degree increment, ranging from 0° to 359°. An example of such table is shown in Fig. 7.

Before any correction is applied to the TCM2 heading, its error can be as large as $\pm 5°$, as shown in Fig. 8 (both clockwise and counterclockwise motion). After a proper deviation table is applied, the error was reduced to $\pm 2°$, as illustrated in Fig. 9.

The final step in the building process is to determine the dc offset of the deviation table since the heading difference between the TCM2 and integrated gyroscope only gives the relative error, not an absolute error.

E. Position Estimation

The navigation system was designed to implement a certain number of features.

1) Because the sensors used by the navigation system do not have the same update frequency and, in the GPS case, do not necessarily update at all, when the AUV is underwater, the position estimator must handle data asynchronously.
2) Between sensor updates, the estimator must be capable of extrapolating in an optimal manner the current states of the vehicle using prior knowledge of the vehicle dynamics and position.
3) Finally, a specific feature of the navigation system is to allow for precise heading alignment at the beginning of a mission. Such a task is necessary in order to reduce the compass-based heading bias, from several degrees of error to a fraction of a degree.

An extended Kalman filter is an ideal candidate for this task, since it satisfies the requirements listed above ([6], [7], [9], [15], [16]).

The Kalman filter proposed herein, which consists of seven states and six measurements, estimates the relative latitude and longitude, local-level ground velocities, heading, heading rate, and, when possible, the heading bias (see Fig. 1 for the linearized state model). When the vehicle is on the surface, the GPS/DGPS measurements dominate the position estimation. Also, when the vehicle moves in a straight direction on the surface, the heading bias becomes observable and can be estimated. This is a very important feature as it can minimize a major source of dead reckoning error. Once the heading bias is precisely known, the vehicle can then dive and perform dead reckoning with very good initial position and heading values. Underwater, the growth in heading error is limited by the fusion of heading and yaw rate measurements.

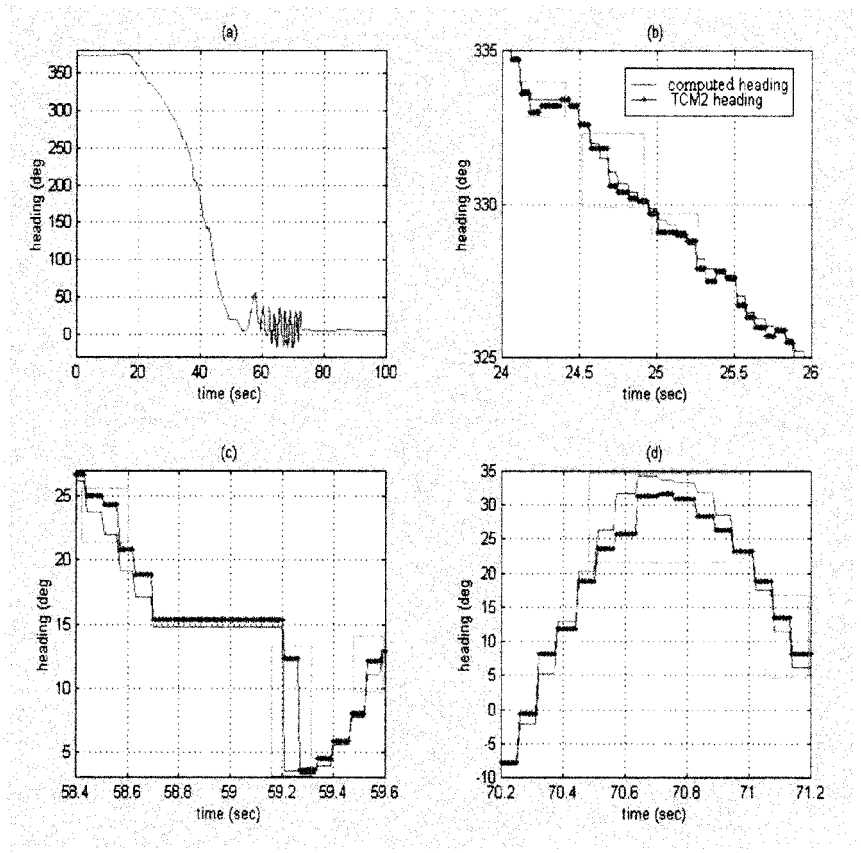

Fig. 6. TCM2 heading versus computed heading.

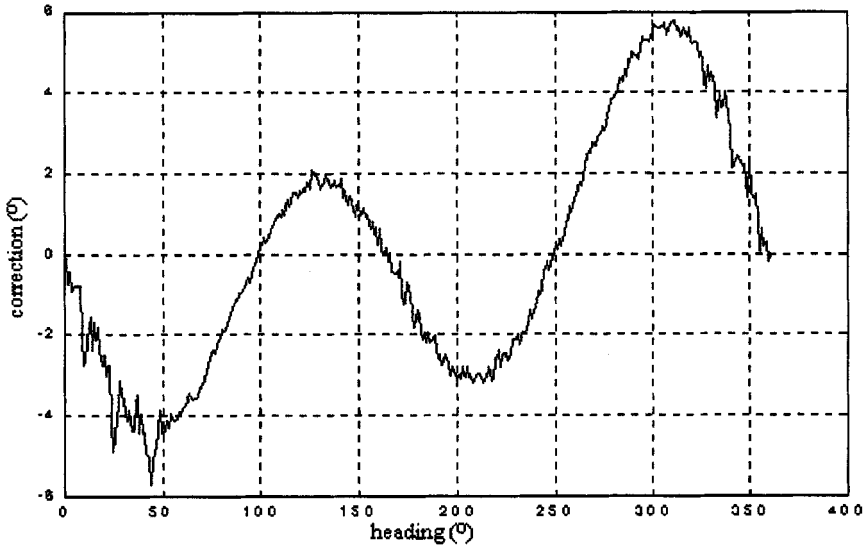

Fig. 7. Deviation table.

It should be noted that, in every filter cycle, not all input data are available because of the different updates and possible dropouts from the sensors. For any of the measurements that do not exist in the current cycle, the corresponding state estimate will not be updated, and the propagation model will be used to update the state estimate.

Optimality of the extended Kalman filter is attained by tuning the matrices that correspond to the model uncertainty and the measurement noise. Theoretically, the components in the diagonal of these matrices represent the error covariance for the corresponding state or measurement. In practice, it is difficult to estimate these covariance coefficients, and the fine-tuning of the matrices often relies on a trial-and-error basis.

IV. Results

The INS system has not yet been physically mounted on the Morpheus at the time of this writing, and the results and anal-

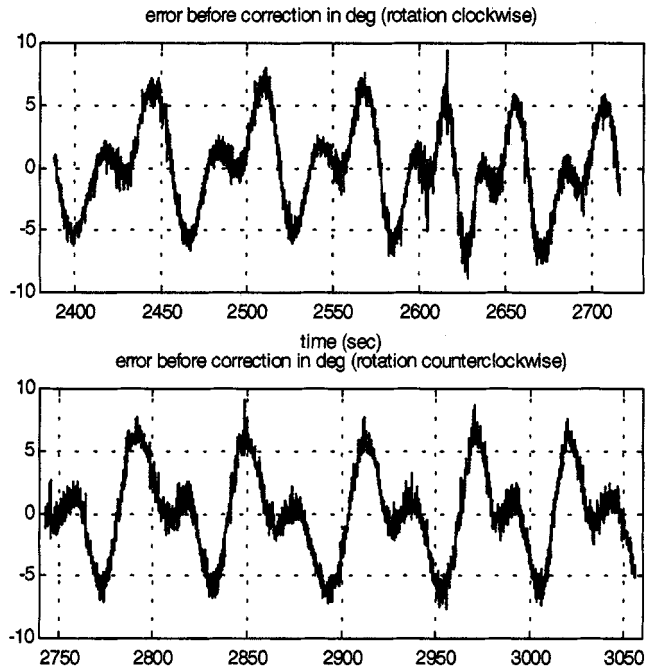

Fig. 8. Heading error.

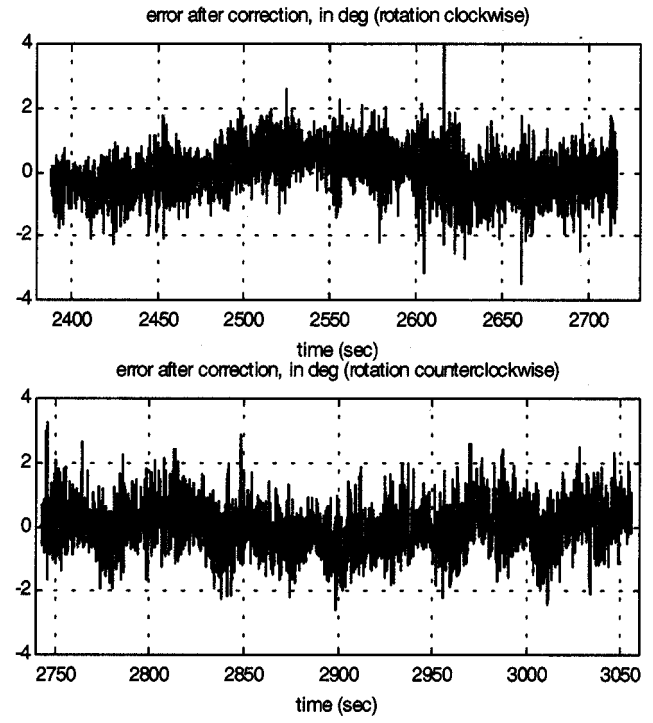

Fig. 9. Heading error after correction.

ysis shown in this section were collected during a mission on June 26, 2000, during which the INS was mounted on an FAU research vessel (R/V Stephan) in order to obtain preliminary at-sea data. In this mission, the outputs of all navigation sensors were logged and postprocessed.

Fig. 10 shows the boat course during the mission, as referenced by DGPS fixes. It first headed north for 2500 m, then east for 2000 m, and finally south for 3000 m, for a total of 7500 m in approximately 1 h.

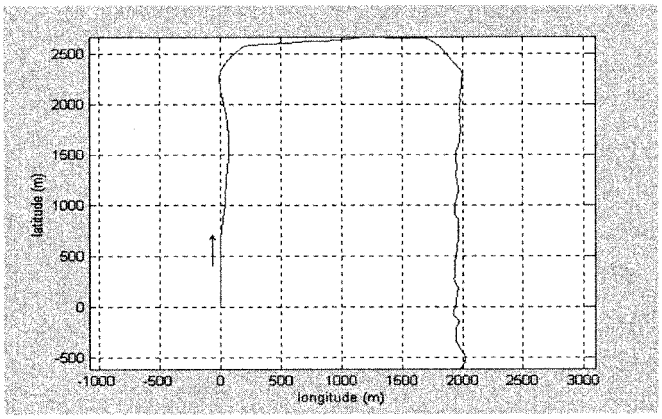

Fig. 10. Boat trajectory.

It is important to understand how the navigation instruments were set up on the boat as it bears implications on how the results should be interpreted. Firstly, there was a considerable level of magnetic signature that arose from the boat itself, and thus the deviation table developed for the compass was not alone satisfactory, as will be seen later. Secondly, the bottom track velocity was updated only at 0.5 Hz as the DVL was programmed to characterize water profiles during the mission. In addition, there were DVL dropouts that occurred during a particular turn in the mission, and certainly these factors will contribute to increased error. Note that these conditions for the preliminary characterization are not considered unreasonable as they represent a fairly realistic scope of what an AUV would encounter during a real survey mission.

The heading profile estimated from the TCM2 compass, after corrected by a deviation table, is displayed on the upper part of Fig. 11, whereas the lower plot shows the difference between the integrated yaw rate output and the corrected compass output. It can be seen that the discrepancy was bounded to within ± 5 degrees.

To characterize the navigation performance, three different data scenarios were compared:

1) All sensor measurements, except the GPS fixes, were used for navigation, namely the ground velocity, the corrected heading, and the yaw rate outputs.
2) Only the ground velocity and yaw rate measurements were fed to the filter. Since the compass data were assumed to be unavailable, the performance for the gyros can be isolatedly evaluated.
3) All sensor measurements were fed to the filter. This configuration allows us to characterize the heading bias estimation performance by the filter.

A. Full Dead Reckoning Mode

Given the yaw rate, heading, and the ground velocity as inputs to the filter, the position error, which is computed as the difference between the filter position output and the DGPS measurements, is shown in Fig. 12.

One can easily notice in the figure that the position error did not increase monotonically, and sharp changes in error occurred when the boat changed its course. As mentioned previously, the

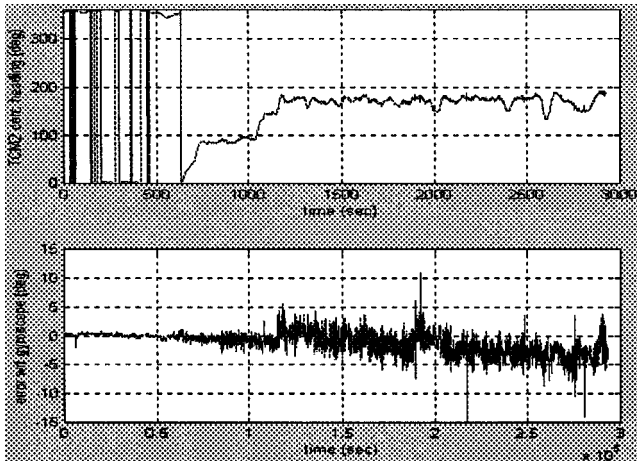

Fig. 11. TCM2 heading after correction.

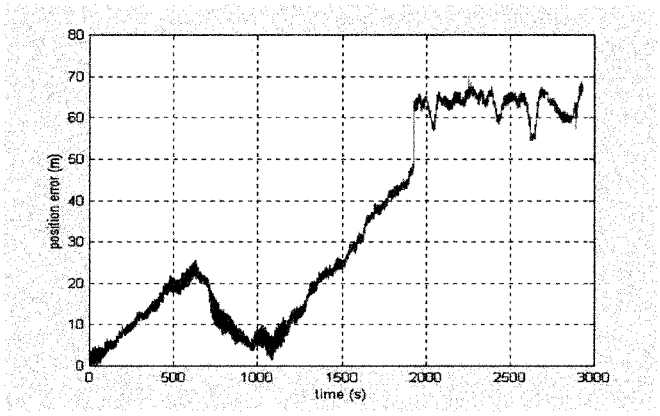

Fig. 12. Position error in full dead-reckoning mode.

deviation table was not able to eliminate the boat's internal magnetic anomaly, and the residual compass error was still quite dependent on the boat's orientation. Thus, when there was a noticeable change in heading, the compass error could be considerably different from that of its previous leg.

At around 1850 s, the position error suddenly increased by approximately 15 m. Note that the sharp change in error was not caused by the compass bias, but by a full 20-s period of DVL dropouts. Since this occurred when the boat was turning 90 degrees south, during which the forward and starboard velocities evolved significantly, it led to both an increase in long-track and cross-track errors. It should be noted that such a long dropout period is considered unusual for routine missions, and the condition considered here can be interpreted as a worst-case maneuvering scenario for the Morpheus.

Despite the compass errors, the overall error was less than 70 m. As the vehicle has traveled an overall distance of 7500 m, the position error amounted to 0.93% of the covered distance. However, this method of quantifying the accuracy of vehicle positioning is highly misleading as it depends very much on the distribution of compass bias throughout the entire 360° orientation. This is evidenced in the first 1000 s, during which the position errors between the north and east legs compensated each other. Had the boat gone north for an hour the error would have been 120 m or more, resulting in a total of 1.5% error of

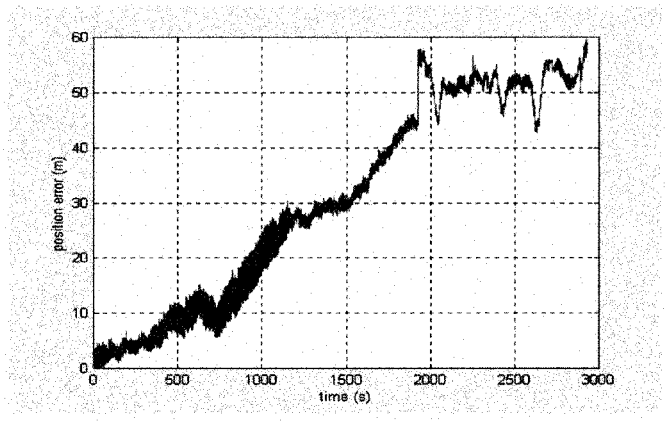

Fig. 13. Position error without compass.

position traveled. It is also very likely that the compass bias could be much larger for some other vehicle's orientation, and the resulting error could have been correspondingly larger if the boat happened to follow those orientations. It is thus more appropriate and less subjective to quantify the position error as a function of only the worst compass bias, although this implies a more tedious and rigorous characterization process. It is thus in the authors' opinions that claiming such positioning accuracy without having any substantial justification will only misinform the AUV community, the end users in particular.

B. Dead Reckoning Without Compass

In this simulation, only the velocity and yaw rate measurements were fed to the filter, and the initial heading value was estimated based on a series of DGPS fixes at the beginning of the mission. The purpose of this test was to characterize the positioning accuracy due to gyro drift.

Fig. 13 shows that the position error increased more consistently as compared to that in the previous case. The overall error was also smaller (less than 60 m). The same sharp change in error at around 1850 s can also be observed in the figure.

The fact that the position error was smaller when the compass data were not used leads to two observations. Firstly, it verifies that the deviation table used in the mission was not very good. More importantly, it shows that the yaw rate measurements can be more reliable than the heading measurements, especially when there are external magnetic signatures, such as bottom mines. Nevertheless, this scenario requires very accurate initial heading information and realignment after some period of time when the gyro drift error becomes excessive. These alignment procedures can be performed online if the heading bias can be estimated.

C. Heading Bias Estimation

In this scenario, all the measurement inputs were fed to the filter. When the vehicle runs a straight segment on surface with continuing DGPS fixes, the heading bias state becomes observable and can thus be estimated. The objective of this scenario is to determine how long it will take the filter to estimate the heading bias to within $\pm 0.2°$ (twice the resolution of the TCM2 compass), as this gives a lower bound on the alignment period (or an overhead of a mission). Ideally, to estimate the heading

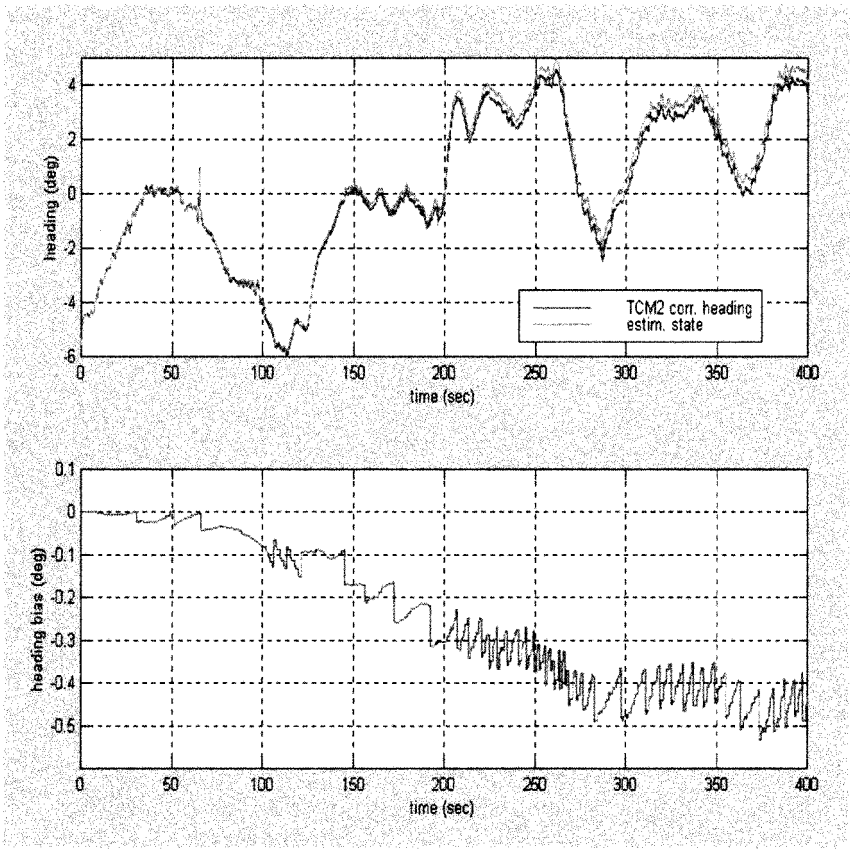

Fig. 14. Heading bias estimation (-0.5° bias).

bias precisely, the vehicle must navigate along a perfectly straight line while acquiring the GPS information. When there are waves and currents, the resulting forcing function plays a dominant role on the heading oscillation (a $\pm 3^\circ$ azimuth wandering for a small vehicle in shallow water is not uncommon). This can result in a large estimation error if the compass bias varies much along that orientation. A useful rule of thumb is to operate on any of the flat spots of the compass deviation curve.

The results shown below are based on the first 7-min data of the mission. Fig. 14 shows a comparison of the corrected TCM2 heading and the heading state in the filter, and the corresponding heading bias estimate. The heading bias successfully converged to within $\pm 0.2^\circ$ at the end of the 6-min period, despite the continuously changing actual heading.

The final heading bias was close to -0.5°. The Kalman filter is thus capable of tracking the heading error efficiently. The overhead, however, is that the AUV must navigate on surface for approximately 7 min, along a direction as constant as possible, to enable the Kalman filter to estimate the heading bias correctly. Such overhead remains acceptable since the resulting gain in terms of navigation accuracy enables the AUV to stay underwater much longer than with an initial heading error of 1°.

Evaluation of the filtering performance is generally difficult to achieve because the true states are in many cases partially or not known. Nevertheless, one can attempt to evaluate the filtering optimality by observing the time history of the one-step ahead prediction errors, which should be white in an ideal case.

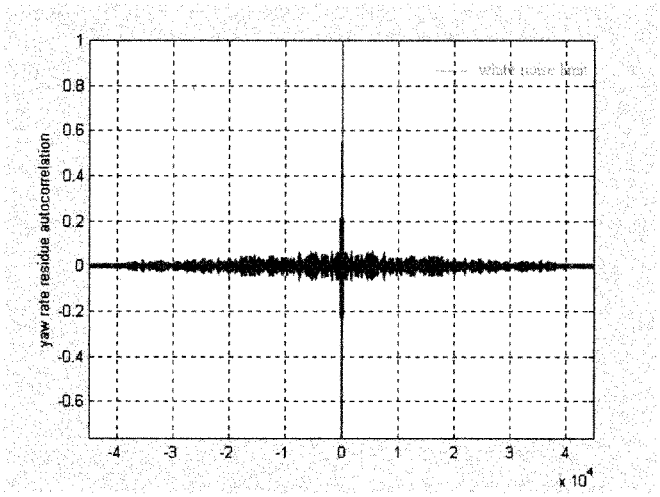

Fig. 15. Yaw rate residue autocorrelation.

In reality, these errors can never be completely white because of the inexact system modeling and sensor noise assumptions. However, the filtering performance can be considered acceptable when the error autocorrelation function falls within a statistically tolerable limit (defined as $\lim_{\text{res}} = 1.96/\sqrt{n}$), where n is the number of samples [5]. Fig. 15 shows an autocorrelation function of the yaw rate one-step prediction errors, overlaid with the statistically tolerable limits. Clearly, the residues are not white, and there is thus a need to further fine-tune the filter

in order to optimize its performance. This will be performed once the INS module is integrated onto the Morpheus.

V. Conclusion

The development and preliminary testing of a Honeywell-based inertial navigation system for the Morpheus vehicle, aided with external DVL and DGPS, have been described. Data processing tools utilized consist primarily of a complementary filter used for attitude estimation and a seven-state extended Kalman filter used for position estimation. The main contribution in this work has been on the development of a low-cost, enhanced navigation system based on thorough characterization of inertial sensors and application of well-founded Kalman theories. Our goal, to be validated, is to achieve a 1% error of position traveled over the duration of an hour. Subsequent realignment will be necessary in order to minimize the accumulated heading error.

Selection of an appropriate IMU depends heavily on the tradeoff between cost and performance requirements, which can vary greatly from one mission/vehicle to another. The development described in this paper capitalized on the low-cost aspect of the Honeywell IMU (as a result of mass production), which is comparable in cost to many of the commercially available solid-state gyros that are not internally compensated. Examples are the Watson Block IMU on FAU Ocean Explorer vehicles [25] and the Systron Donner IMU on the Naval Postgraduate School Phoenix vehicle [27].

The extended Kalman filter encompasses three important features: 1) it allows for asynchronous sensor update rates and sporadic drop-outs; 2) it uses GPS/DGPS fixes whenever they are available to estimate the vehicle position and heading bias; and 3) it does not have any states to account for Doppler biases because the body-fixed ground speed measurements are typically much more accurate (0.2% of speed traveled). Preliminary filtering results indicate that the convergence of the heading bias estimate took approximately 7 min given that the vehicle cruised along a straight line on surface with steady DGPS fixes.

A substantial amount of effort has been spent on characterizing the TCM2 compass in terms of pitch, roll, and heading, and its inherent heading error was found to be within 2 degrees (approximately 3.5% error of position traveled). As the heading error based on any magnetic compass is sensitive to the vehicle's orientation, the positioning performance should be characterized in terms of the worst heading deviation, or misleading conclusions can easily be drawn. In our future implementation, the TCM2 will be used only for initializing the heading estimate in the filter.

To further improve the accuracy of the system, we will investigate two additional methods that might reduce the rate bias error inherent in the measurement. Firstly, we are examining the performance of an augmented filter which has the yaw rate bias as an extra state. In parallel, a separate, three-state (heading, yaw rate, and yaw rate bias) Kalman filter will also be studied. These two filter configurations will be compared, and tradeoffs between estimation performance and filter size will be discussed in our future paper.

References

[1] B. Allen, R. Stokey, T. Austin, N. Forrester, R. Goldsborough, M. Purcell, and C. Von Alt, "Remus: A small low cost AUV: System description, field trials and performance results," in *Proc. Oceans'97*, NS, Canada, Sept. 1997, pp. 994–1000.

[2] P. E. An and M. Dhanak, "Regional oceanography using a small AUV," in *Proceedings UUV Showcase 98*, U.K.: Southampton Oceanography Center, Sept. 1998, pp. 119–129.

[3] D. Atwood, J. Leonard, J. Bellingham, and B. Moran, "An acoustic navigation system for multi-vehicle operations," in *Proc. 9th Int. Symp. of UUST*, Durham, NH, Sept. 1995, pp. 202–208.

[4] N. Barbour and G. Schmidt, "Inertial sensor technology trends," in *Proc. AUV Navigation Workshop*, Boston, MA, 1998, pp. 55–62.

[5] S. Billings and W. Voon, "Correlation based model validity tests for non-linear models," *Int. J. Control*, vol. 44, no. 1, pp. 235–244, 1986.

[6] W. L. Brogan, Ed., *Modern Control Theory*, 3rd ed. Englewood Cliffs, NJ: Prentice-Hall, 1991.

[7] R. Brown and P. Hwang, Eds., *Introduction to Random Signals and Applied Kalman Filtering*. New York: Wiley, 1997.

[8] T. Curtin, J. Bellingham, J. Catipovic, and D. Webb, "Autonomous oceanographic sampling network," *Oceanography*, vol. 6, no. 3, pp. 86–94, 1993.

[9] A. Gelb, *Applied Optimal Estimation*. Cambridge, MA: MIT Press, 1986.

[10] D. Gibson, "3D vector processing of magnetometer and inclinometer data," *Cave Karst Sci.*, vol. 23, no. 2, pp. 71–76, 1996.

[11] G. Grenon, E. An, and S. Smith, "Enhancement of the inertial navigation system of the Florida Atlantic University autonomous underwater vehicles," in *Proc. Underwater Technology Conf.*, Tokyo, Japan, May 2000, pp. 413–418.

[12] G. Grenon and E. An, "A complementary filter for pitch and roll angle estimation on the MiniAUV," Ocean Engineering, Florida Atlantic Univ., Dania, FL, Internal AUV Rep., Dec. 1999.

[13] G. Grenon, "Precision navigation TCM2 compass—Compensation of heading error by means of a deviation table," Ocean Engineering, Florida Atlantic University, Dania, FL, Internal AUV Rep., June 1998.

[14] J. Huddle, "Trends in inertial systems technology for high accuracy AUV navigation," in *PROC. AUV Navigation Workshop*, Boston, MA, 1998, pp. 63–73.

[15] R. E. Kalman, P. L. Falb, and M. A. Arbib, *Topics in Mathematical Theory*. New York: McGraw-Hill, 1969.

[16] P. S. Maybeck, "The Kalman filter: An introduction to concepts," in *Autonomous Robot Vehicles*. Berlin, Germany: Springer-Verlag, 1990, pp. 194–204.

[17] H. Medwin, "Speed of sound in water for realistic parameters," *J. Acoust. Soc. Amer.*, vol. 58, p. 1318, 1975.

[18] B. Parkinson and J. Spilker, Eds., "Global positioning system: Theory and application," in *Progress in Astronautics and Aeronautics*: AIAA, 1996, vol. vol. 163&164.

[19] "TCM2 Electronic Compass Module—User's Manual," Precision Navigation, Inc., Sept. 1, 1997.

[20] H. Schmidt, J. Bellingham, M. Johnson, D. Herold, D. Farmer, and R. Pawlowicz, "Real-time frontal mapping with AUV's in a coastal environment," in *Proc. Oceans'96*, Ft. Lauderdale, FL, Sept. 1996, pp. 1094–1098.

[21] S. Smith and E. An, "Morpheus: Ultra modular AUV for coastal survey and reconnaissance," in *Proc. UUVS'00*, Southampton, U.K., Sept. 2000.

[22] S. M. Smith, P. E. An, J. Park, L. K. Shay, H. Peters, and J. Van Leer, "Sub-mesoscale coastal ocean dynamics using autonomous underwater vehicles and HF radar," in *Proc. 2nd Conf. Coastal Atmospheric and Oceanic Prediction and Processes*. Phoenix, AZ: Amer. Meterol. Soc., Jan. 1998, pp. 143–150.

[23] S. M. Smith, K. Ganesan, P. E. An, and S. E. Dunn, "Strategies for simultaneous multiple AUV operation and control," *Int. J. Syst. Sci.*, vol. 29, no. 10, pp. 1045–1063, 1998.

[24] S. M. Smith, J. Park, J. Rivero, T. Pantalakis, E. Henderson, and E. An, "Development of hydrographic survey capabilities on the Ocean Explorer AUV," in *Proc. Oceanology Int. Conf.*, vol. 2, Brighton, U.K., Mar. 1998, pp. 109–118.

[25] S. M. Smith, K. Heeb, N. Frolund, and T. Pantelakis, "The Ocean Explorer AUV: A modular platform for coastal oceanography," in *Proc. 9th Int. Symp. UUST*, Durham, NH, Sept. 1995, pp. 67–73.

[26] S. M. Smith and S. E. Dunn, "The Ocean Voyager II: An AUV designed for coastal oceanography," in *AUV 94*, Boston, MA, Sept. 1994, pp. 139–147.
[27] B. M. Stinespring, "The experimental evaluation of a DGPS based navigational system for the Aries AUV," Master thesis, Naval Postgraduate School, Monterey, CA, p. 29, June 2000.
[28] X. Yun *et al.*, "Testing and evaluation of an integrated GPS/INS system for small AUV navigation," *IEEE J. Oceanic Eng.*, vol. 24, pp. 396–404, July 1999.

Gabriel Grenon received the undergraduate degree from the Université de Technologie de Compiègne, Compiègne, France, in 1998, and the M.S. degree in engineering from Florida Atlantic University, Dania, FL, in 2000.

His research specializes in robotics and automation, and particularly in autonomous underwater vehicle navigation. He is currently a software engineer for the Department of Ocean Engineering at Florida Atlantic University..

P. Edgar An received the B.S.E.E. degree from the University of Mississippi, University, in 1985, and the M.S.E.E. and Ph.D. degrees from the University of New Hampshire, Durham, in 1988 and 1991, respectively.

After completing his doctoral work, he became a Post-Doctoral Fellow in the Department of Aeronautics and Astronautics at the University of Southampton, Southampton, U.K., working on the European Prometheus project. In 1994, he joined the Department of Ocean Engineering at Florida Atlantic University (FAU), Dania, as a visiting faculty member. He became an Assistant Professor at FAU in 1995, and is currently an Associate Professor. His areas of interest are autonomous underwater vehicles, navigation, control, modeling and simulation, and neurofuzzy systems. His publications include more than 50 journal and conference papers in these research areas.

Dr. An is a recipient of the 1998 FAU Researcher of the Year award for the Assistant Professor level. He is a member of Sigma Xi.

Samuel M. Smith received the Ph.D. degree in electrical and computer engineering from Brigham Young University, Provo, UT, in 1991.

He is President of Adept Systems, Inc., Boca Raton, FL, and currently located at Orem, UT. He is also a part-time faculty member in the Electrical and Computer Engineering Department at Brigham Young University. He was formerly a Professor of Ocean Engineering, Florida Atlantic University, Dania, and Director of the Advanced Marine Systems Lab. His general research interests include autonomous underwater vehicles, automation systems, intelligent control systems, intelligent distributed control and sensing systems, fuzzy logic control and decision making, automated reasoning, and signal processing. He is currently conducting research in the areas of survivable naval shipboard automation systems and component-level intelligent distributed automation infrastructures.

Anthony J. Healey received the undergraduate degree from Kings College, London University, U.K., and the Ph.D. degree in mechanical engineering from the university of Sheffield, U.K., in 1966.

His specialty is in dynamic systems and control. He has taught at the Pennsylvania State University, the Massachusetts Institute of Technology, and the University of Texas at Austin. For five years, he worked with Brown and Root, Inc., Houston, TX, and has been Chairman of the Mechanical Engineering Department of the Naval Postgraduate School, Monterey, CA, from 1982 to 1992. He is currently a Professor in the Mechanical Engineering Department and Director of the Center for AUV Research, with the aims of developing AUV technology for naval applications of AUVs. He is responsible for the development of the Phoenix Autonomous Vehicle and for the graduation of numerous Master's and Ph.D. students, many working on AUV-related topics. He has authored over 120 papers and publications.

Prof. Healey is a member of the IEEE Oceanic Engineering Society and has been involved in the organization of the IEEE AUV series of conferences, Office of Naval Research workshops on Fault Detection, and Modeling and Simulation for Multi Robot Systems in Mine Countermeasures. He is a member of the American Society of Mechanical Engineers (ASME). He is listed in *Who's Who in Engineering* and was awarded a Dedicated Service Award by the ASME in 1994.